Jurnal
Teknologi

Review Paper

OPTIMIZING FLAME SYNTHESIS OF CARBON NANOTUBES: EXPERIMENTAL AND MODELLING PERSPECTIVES

Muhammad Thalhah Zainal, Mohd Fairus Mohd Yasin*, Mazlan Abdul Wahid

High Speed Reacting Flow (HiREF) Laboratory, Universiti Teknologi Malaysia, 81310 UTM Johor Bahru, Johor, Malaysia

Article history
Received
1 January 2016
Received in revised form
18 May 2016
Accepted
15 June 2016

*Corresponding author
mohdfairus@fkm.utm.my

Abstract

Synthesis of carbon nanotubes in flames has become highly attractive due to its rapid, inexpensive, and simple method of production. The study of flame synthesis of carbon nanotubes revolves around the control of flame and catalyst parameters to increase the synthesis efficiency and to produce high quality nanotubes. The control parameters include flame temperature, concentration of carbon source species, catalyst type, equivalence ratio, and fuel type. Carbon nanotubes which are produced with rapid growth rate and possess high degree of purity and alignment are often desired. The present study reviews various optimization techniques from the advanced studies of chemical vapour deposition which are applicable for the synthesis of nanotubes in flames. The water-assisted and catalyst free synthesis are seen as possible candidates to improve the growth rate, alignment, and purity of the synthesized nanotubes. The state-of-the-art of the flame synthesis modelling at particle and flame scales are reviewed. Based on the thorough review of the recent experimental findings related to the catalytic growth of nanotube, possible refinement of the existing particle scale model is discussed. The possibility of two-way coupling between the two scales in computational fluid dynamics may be a major contribution towards the optimization of the flame synthesis.

Keywords: Carbon nanotube; flame synthesis; modeling

Abstrak

Penghasilan tiub nano karbon melalui pembakaran semakin mendapat perhatian memandangkan kaedah penghasilannya cepat, murah, dan ringkas. Kajian tentang penghasilan tiub nano karbon melalui pembakaran menjurus ke arah meningkatkan mutu tiub nano karbon dan tahap kecekapan proses penghasilannya dengan cara mengawal parameter api dan bahan pemangkin. Parameter yang boleh dikawal termasuklah suhu api, kepekatan spesis sumber karbon, jenis bahan pemangkin, nisbah setara, dan jenis bahan api. Tiub nano karbon yang dihasilkan dengan kadar pertumbuhan yang tinggi serta bersih dan sejajar seringkali dikehendaki. Kajian ini mengulas pelbagai teknik untuk mengoptimumkan penghasilan tiub nano karbon yang terdapat dalam kaedah pemendapan wap kimia yang juga dilihat boleh diaplikasikan dalam kaedah penghasilan melalui pembakaran. Teknik bantuan air dan penghasilan tanpa bahan pemangkin dikenalpasti antara kaedah-kaedah yang baik untuk meningkatkan kadar pertumbuhan, kesejajaran, dan kebersihan tiub nano karbon. Kajian ini juga akan mengulas model terkini berkaitan penghasilan tiub nano karbon melalui pembakaran pada skala partikel dan skala api. Berdasarkan ulasan terperinci daripada penemuan-penemuan ujikaji berkaitan penghasilan tiub nano karbon berpemangkin, kebarangkalian untuk menambahbaik model partikel yang sedia ada akan dibincangkan. Kemungkinan menyatukan kedua-dua skala dalam keadaan dua hala melalui kaedah pengiraan dinamik bendalir dilihat berupaya memberikan sumbangan dalam mengoptimumkan penghasilan tiub nano karbon melalui pembakaran.

Kata kunci: Tiub nano karbon; penghasilan melalui pembakaran; pemodelan

1.0 INTRODUCTION

Since the discovery of carbon nanotubes (CNT) by Iijima in 1991 [1], tremendous research has been conducted to explore the field of CNT. In general, CNTs could be classified into single-walled CNT (SWCNT) and multi-walled CNT (MWCNT), the former offers better properties than the latter. CNTs of different qualities are needed in various applications due to their incredible mechanical and electrical properties [2–6]. Perfectly aligned CNTs with high purity

are required to produce the desired electrical properties in electronics industry [7] while lower quality CNTs may offer an economical solution to produce good mechanical properties in composite industries [8–10]. CNTs have significant contribution in the medical field such as cancer treatment, enhancement of biosensors, drug transport, and tissue engineering, where pure and aligned SWCNTs are often preferred [11–15].

The most common methods of producing CNTs are arc discharge, laser ablation, flame synthesis, and chemical vapour deposition (CVD). The CVD is a well-established method for mass production where countless studies have been done. However, flame synthesis is emerging as a challenger despite lacking in both theoretical and modelling aspects. Unlike other methods which use an external heater that is separate from the carbon source stream, the flame synthesis produces both the heat and carbon source species from the fuel itself. Once the flame is ignited, both heat and carbon source are simultaneously generated and an optimum temperature for the synthesis is automatically produced [16]. Besides, flame synthesis is a rapid process and does not require expensive tools with high energy consumption. Owing to these simple and cost-effective features, flame synthesis offers an economical solution for mass production of CNT [17]. However, a lot of effort is still needed to improve CNTquality and to optimize CNT production in flames. CNT quality could be characterized in terms of purity, alignment, tip condition, and number of walls. The present study discusses optimization objectives for mass production of CNT in flames which are the CNT qualities and the CNT growth rate.

Previous studies of CNT synthesis in flames relied heavily on experimental works while modelling studies were very few [18]. Most experimental studies on flame synthesis with different flame and catalyst configurations have been done without a systematic optimization attempt. Therefore, computational studies are essential to reduce the number of experiments in optimizing the complex processes in flame synthesis. Several review papers have been published on flame synthesis but are mainly focused on the experimental side with no detail discussion about computational work. Merchan-Merchan et al. [17] produced a comprehensive review on flame synthesis without a clear conclusion about a successful optimization attempt. Recently, Mittal et al. [19] reviewed various experimental works on premixed and diffusion flame synthesis and discussed some modelling works in their review paper. A review on optimization techniques for aligned CNT synthesis was given by Seah et al. [20]. Although optimization for flame synthesis was included, the review only concentrates on CVD. To the best of our knowledge, no review has been done on the modelling and optimization of CNT in flame synthesis, which is the main focus of the present paper.

In section 2, previous experiments on flame synthesis of CNT will be briefly described along with optimization strategies from advanced CVD studies. Section 3 is dedicated to the modelling aspect of CNT growth in flames.

2.0 EXPERIMENTAL STUDIES ON FLAME SYNTHESIS OF CARBON NANOTUBES

Flame synthesis experiments could be categorized into premixed and diffusion flames. Previous studies on premixed flame configurations include the normal premixed flame and the burner with wall stagnation flow. In the case of diffusion flame, three flame setups have been widely used which are normal diffusion flame, inverse diffusion flame, and counter flow diffusion flame. Each flame configuration has its own merits. Inverse diffusion flame which results in carbon precursors outside the flame sheet [21] and counterflow diffusion flame with simple geometry provides a convenient sampling process [16]. Premixed flame enables a unique control over the equivalence ratio [19] and provides a large surface for CNT growth on a plate at the exit of the burner with wall stagnation flow [22,23].

2.1 Flame and Catalyst Parameters That Govern Flame Synthesis

The operating parameters in flame synthesis studies include flame temperature, fuel source, type of catalyst, and sampling region [19,24]. In premixed flame configurations, flame stretch rate and equivalence ratio are additional parameters of study [23]. Fuels such as ethylene, acetylene, methane, propane, and polyethylene are frequently used due to the fuel oxidation path which is favourable for the carbon source species. Some researchers have used mixed fuels with synthesis product of onion-shaped nano-structures [25,26] and others have used alcohol-based fuel [27]. Fuel source is frequently mixed with inert gas diluent to achieve the desired fuel concentration and to remove encapsulating layers on catalyst surface [16,28]. While nitrogen is commonly used as diluent gas, argon and helium are also reported by some authors [24,29].

Iron, nickel, and their alloys or metallocene are identified as appropriate catalyst material. Catalyst particles could be introduced into premixed flames either by aerosol mechanism [29–31], or by substrate coating [32–34]. For substrate coating, catalyst particles are typically deposited on stainless steel mesh grids [27,33]. In other studies, the catalyst material itself is formed into a substrate in the shape of meshes [25], rods [35] or wires [36–38]. Less common materials such as metal-oxide spinels was used by Memon [39,40]. The collection time for aerosol-based catalyst is more rapid in the range of milliseconds [24,41] compared to the substrate-based catalyst which may be completed within several minutes [25,27,42].

In premixed flames, the sampling region where the CNT growth takes place usually lies at few centimetres above the burner along the flame axial direction [32,34]. In diffusion flames, growth region is usually observed closer to the burner in the order of 10mm height above burner. Growth in radial direction was reported by authors of premixed wall stagnation flow burner in the order of 10mm from the central axis of the flame [22,23]. The optimum temperature for CNT growth in flames, generally measured at substrate surface, typically lies within 1000-1200K. Nevertheless, some experiments including wall stagnation flow burners recorded temperatures lower than 1000K [42–44].

In the case of premixed flames, effect of equivalence ratio and strain rate could be considered. Most studies use rich flame with equivalence ratio (φ) in the range of $\varphi = 1.4 - 1.8$ [24,27,32,34] although $\varphi > 2$ [33] was reported elsewhere. Rich flames is often preferred since it provides high concentration of carbon precursors for CNT growth [45]. The range of flame strain is dependent on the equivalence ratio [23]. Nevertheless, additional studies to support the findings on flame strain rate might be needed since studies on such specialized area in nanotube production is less frequently published.

2.2 Quality of Flame Synthesis for CNT Production

CNT output could be characterized with regards to its physical features and the tube quality. Ideally, the synthesized CNTs should have high growth rate with small diameters (SWCNT), long and straight tube, and are free from contaminants. Growth rate is an important parameter in synthesis process. Fast CNT growth with long catalyst lifetime indicates the feasibility of mass production. CNT growth rate could be expressed by the ratio between the increase in the tube length ΔL_{CNT} and the growth period Δt [41], as shown in equation (1).

$$r_{growth} = \Delta L_{CNT}/\Delta t \quad (1)$$

Vander Wal et al. [28] estimated 0.2-2μm/s growth rate through observation of catalyst dwell time inside the CNT formation region. A similar approach was used by another study [46] which utilized computational fluid dynamics to compute CNT growth rate in CVD reactor. A growth rate of over 100μm/s was recorded by combining measurements of flame speed and CNT length [30,41]. The application of flame speed measurement in the growth rate calculation may have introduced a large uncertainty which result in the large discrepancy with other reported values of growth rate measurement.

MWCNTs were observed for most premixed flame configurations, exhibiting lengths of several to tens of micrometers [27,33,47] and diameters up to 90nm [22,32,33]. SWCNT is not frequently reported and have smaller diameters than that of the MWCNT up to 5nm [24,29,48]. CNTs that are entangled, coiled and bent were most frequently reported. Premixed flames have shown the capability to synthesize aligned MWCNTs to a great degree of parallelism [27,34] though the formation of pure nanotubes in premixed flames is rarely reported. Nakazawa et al. [22] reported pure CNT formation in double wall stagnation flow burner which is attributed to the optimal temperature and species concentration though the actual mechanism that controls purity remained unclear. The present study concludes on the purity level from the electron microscope images of respective studies when the purity level is not mentioned. Impurities on the CNTs include the soot layer on the tube surface [27], metal catalyst nanoparticles at tips and tube surface [23,33,34], irregular tube surfaces [47], and soot mixing with the tubes [23].

Studies on diffusion flames report CNT length similar to that found in premixed flames (in the order of 100 nm to 1μm with exceptionally long tubes of 10μm to 40μm length. MWCNTs are more frequently produced compared to that of SWCNTs, which was achieved in just a few experimental works [21,28,30,39–41] besides other types of nanostructures like branched CNTs [38], bamboo-shaped CNTs [49], and carbon nano-onions [25]. The synthesis of CNTs in diffusion flames are mostly by electrical field control [35,37,38] though another study produced highly aligned CNTs without the assistant of electricity in normal diffusion flame and counterflow diffusion flame using anodic aluminum oxide template with nano-sized pores [44]. Similar to premixed flames, formation of pure CNT in diffusion flames is also rarely mentioned. Merchan-merchan et al. [37,38] observed the absence of soot particles and non-tubular structure within the CNTs formed in counter diffusion flame. Many experimental works on CNT synthesis in diffusion flames have reported CNT impurities in the form of clinging catalyst particles, encapsulation of aromatic carbon particles and soot agglomeration [21,23,27,29,30,42,43].

2.3 Optimization Strategies for Flame Synthesis

The influential parameters and the synthesis product of different flame configurations have been discussed in the previous section where it can be inferred that more efforts are needed to enhance flame synthesis output in terms of purity, alignment, and growth rate. In this section, CVD studies were cited primarily because their catalytic growth mechanism is similar to that of the flame synthesis [44]. Having better experimental and modelling development compared to the flame synthesis, CVD studies may be referred to explore various optimization strategies in flame synthesis.

2.3.1 Water-Assisted Synthesis

Recently, water has been proved to assist a rapid growth of CNT [20] by acting as an etching agent for catalyst surfaces that are covered by deposited amorphous carbon [50,51]. Removal of amorphous

carbon provides clear catalyst surface and indicates enhanced CNT growth and catalyst lifetime. Another effect of water is to resist the clustering of catalyst particles due to deposition of small particles on the surface of large ones, a phenomena known as Ostwald ripening [52,53] which leads to catalyst deactivation.

Water could be incorporated during CNT synthesis by passing it into a hot furnace at certain amount and pressure [54]. Amama et al.[53] injected water into the reaction chamber during substrate annealing and Liu et al. [55] incorporated water into the synthesis chamber by passing inert carrier gas into a mixing tube containing water vapour before the entrance of the chamber. Another study introduced water into the CVD furnace by preparing water-embedded catalyst material called aerogels [56]. Astounding growth rate of more than 4.17μm/s has been reported [57] with high CNT purity [58]. The growth rate of water-assisted CNT synthesis in CVD furnace is a factor of 2 higher compared to that of the previous flame synthesis using diffusion flame [28,29] though another flame synthesis which measured the growth rate based on the flame speed produced a two order of magnitude higher growth rate [30,41] compared to the former. Zhu et al. [50] produced multiple layers of pure CNT through water-assisted process where as grown CNTs had their caps at the tube end removed and new layers of CNT are synthesized from the loose tip. This phenomenon is attributed to the excellent etching effects of water, which also explains the CNT walls that are free from particles.

Water-assisted experiments described previously are done in CVD reactors [50,53–56]. Owing to the similar growth mechanism between CVD and flame synthesis, water-assisted experiments is likely to be applicable in flame synthesis. Water may be introduced in flame environment in the form of mist spray which is a common technique for NOx suppressant that reduces flame front temperature [59]. Etching effects of water in flame synthesis has been mentioned by several authors [34,44], but the observation was on the effects of water as a combustion product rather than a component of the reactant mixture. A successful application of water in flame synthesis as purifying agent and catalyst poisoning suppressant may lead to high yield and high quality flame synthesis at low cost in the future.

2.3.2 Self-Catalysed & Catalyst-Free Synthesis

Self-catalytic synthesis of CNT in combustion environment may be viewed as a synthesis technique where old CNTs are treated as growth sites for new CNTs. This technique allows the synthesis to be free from impurities which are introduced by the use of foreign particles. A previous experimental study demonstrated the self-catalytic synthesis of CNTs through detonation [60]. Though the supersonic burning speed which is found in detonation environment cannot be produced in laminar flame, the study proves the possibility of self-catalytic process under certain favourable condition. The CNTs which were synthesized by CVD method and treated with nitric and hydrochloric acid solution were used as growth sites to produce clean and straight CNTs. Later in 2009, Woo et al. reported self-catalytic behaviour of CNTs where pre-synthesized CNTs from premixed flames were treated with a similar acidic solutions before being reused as the new growth sites [23]. However, the description on the self-catalytic mechanism in flame remains unclear and are yet to be supported by other studies before one could draw conclusions about the self-catalysed flame synthesis.

Catalyst-free synthesis has been used by some researchers to reduce cost of production by avoiding the expensive after-treatment of CNT. MWCNT forest was produced on aluminium substrate without catalyst coating [61]. The substrate is placed under reduction-oxidation treatment before synthesizing CNTs in the reaction chamber. Merchan-Merchan et al. claimed that in the absence of catalyst particles, the CNT growth is still possible in an oxygen-enriched environment [62]. The absence of catalyst in flame synthesis was also reported by Lee et al. [43] where only carbon nanofibers are formed on bare substrates with low growth rate.

2.3.3 Catalyst Pattern on Substrate

CNT alignment could be enhanced by catalyst patterns on substrate such as pores and scratches [63–65]. Martin et al. deployed zeolite substrates in a CVD synthesis and capitalized its unique porous geometry to control the location, direction and density of CNT growth [63]. To the best of our knowledge, the use of zeolites as catalysts has not been reported in flame synthesis. The closest resemblance is the use of anodic aluminum oxide layer [44] that features zeolite-like porous surface. Liu et al. grew SWCNTs along scratches on silicon dioxide (SiO_2) substrate [65]. Nano-sized lines were non-uniformly carved on the substrate surface using SiO_2 atomic force microscopy tips which is attractive due to the simplicity and the ease of control over CNT density on a substrate.

2.3.4 Aerosol Catalyst for Continuous Production

Continuous production is one of the challenges in mass production of CNT. Production is inefficient by the batch process where catalyst-coated substrate needs to be prepared repetitively. To overcome this problem, aerosol-type catalyst particles could be entrained continuously into flame environment via a bubbler or a direct method [21,29–31,48]. Since aerosol-type catalyst does not involve substrate preparation, a continuous production is possible. The control over CNT morphology and alignment might be difficult with aerosol-type catalyst due to the random dispersion of particles in flames. Nevertheless, for applications that could compromise CNT alignment such as material composites, aerosol catalyst is likely the way forward for the mass production.

2.3.5 Other Optimization Methods

The control over some parameters such as temperature and pressure results in desired CNT shapes. A study by Simon et al. [66] showed that reaction temperature played an important role for the transition from fibrous to tubular nano-structure. Previous study has shown that the increase in temperature of catalyst particles causes carbon atoms to have higher mobility to diffuse through catalyst particle which results in the increase of growth rate [67]. Borowiak- Palen et al. [68] found that CNT morphologies could be controlled by the pressure of the feed stock. They claimed that pure SWCNT and MWCNT could be formed at low and high pressures respectively. Another study by Park and co-workers [69] reported the positive effects of pressure on CNT structural features such as CNT crystallinity, length, and density.

Cost-effective and conveniently available fuel source such as alcohol or liquefied petroleum gas (LPG) may reduce the cost of CNT production. Some authors have shown successful CNT growth using alcohol and LPG [70–72]. Huang et al. managed to produce CNT forests from the LPG fuel in a CVD reactor [72]. One study went further on reducing CNT production cost by utilizing natural herbs as catalyst along with the LPG fuel [73]. Despite the sulphur content envisioned to poison catalyst particles, LPG carbon precursors are able to produce packed and long CNTs with small diameters [71,72]. There are limited studies on the use of alcohol, LPG, and alternative fuels for CNT synthesis in flames [74–76] which may be explored to capitalize on their economic benefits.

Application of voltage bias has shown the capability of producing CNTs with enhanced electrical properties. Tsai et al. [77] observed the effect of voltage bias on the formation of multi-branched CNTs in Microwave Plasma Enhanced CVD. The unique structure of multiple-branched CNTs is believed to exhibit excellent electrical properties such as conductivity and field emission properties [78]. Multi-branched CNTs were also reported in voltage-assisted flame synthesis by Merchan-Merchan [38] who suggested a rather similar theory of voltage impact on the melting of nanoparticles. Ngo et al. [79] utilized plasma enhanced CVD to produce aligned carbon nanofibers with the motivation of enhancing chip fabrication architecture. The enhancement of the electrical properties of carbon nanofibers is produced by small cone angles which are observed on elongated catalyst particle during melting [79].

Thus far, various techniques to optimize CNT production have been presented. Optimizing many parameters that affect CNT growth in the experiment would be very costly and time-consuming. Modelling studies are required to save experimental time and cost of CNT characterization. At present, accurate optimization using computational tool requires further refinement of the present models. Therefore, the next section is dedicated on the review of modelling studies for CNT synthesis that could be applied in flame environments.

3.0 MODELING OF CARBON NANOTUBES

CNT synthesis in flames occurs at two different scales which are the flame and the particle scales. The reacting flow dynamics that occurs at the flame scale are captured by the transport equations of mass, momentum, and energy that are solved simultaneously with the chemical kinetics of fuel oxidation. The computation is done within the computational fluid dynamics (CFD) framework. At the particle scale, the interaction between catalyst particles and carbon precursors, CNT nucleation, CNT growth, and catalyst deactivation are captured by the growth rate model which will be discussed in section 0. Multi-scale modelling that couples the two scales together is needed to accurately predict the catalytic CNT growth in flames.

3.1 Particle-Scale Modelling

The model development at particle scale is needed to predict the growth rate of CNT and the catalyst particle formation for aerosol type catalyst which involves a phase change. The experimental finding which involves the in-situ measurement of catalytic growth of CNT within a controlled environment is explained in the present section to provide the chronological background of the model development and the possible future refinement of the present models.

3.1.1 Growth Rate Model

Activities at particle scale start as early as the decomposition of hydrocarbon molecules and catalyst metal into carbon atoms and nanoparticles respectively [46]. A well accepted chronology leading to CNT formation starts from the deposition of carbon atoms on catalyst nanoparticle, then the diffusion of carbon atoms into the nanoparticle followed by the CNT nucleation from within the nanoparticle [28]. In most cases, amorphous carbon layers eventually encapsulate the catalyst particle which disables carbon atom diffusion and hence CNT growth.

Several researchers have attempted to model and determine CNT growth rate. Wen et al. [45] calculated growth rate of single-walled nanotubes using the change in CNT length over time, as shown in equation (2).

$$dL_{CNT}/dt = \left(m_C/\pi\rho_c\delta_{gr}d_{CNT}\right) dN_{CNT}/dt \quad (2)$$

The variables m_C, ρ_c, δ_{gr}, d_{CNT}, and N_{CNT} denote the mass of carbon atom, the density of carbon atom, the thickness of graphene layer, the diameter of the synthesized single–walled CNT, and the number of

carbon atom which contributes to the growth of CNT respectively.

A catalytic growth rate model which was derived from the diamond nucleation in CVD by Liu and Dandy [80] was provided by Zhang and Smith [81] as shown in Figure 1.

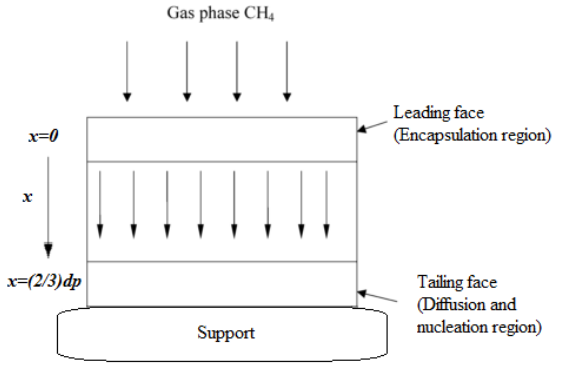

Figure 1 Illustration of CNT growth model developed by Zhang and Smith [81]. Adapted from [81].

The model depicts the leading face at $x = 0$ on catalyst surface where the interaction between carbon precursors and catalyst takes place. The CNT growth happens on the tailing face at $x = (2/3)d_p$ where $d_p$is the particle diameter. The gas-phase carbon precursors would first come in contact with the leading face, decompose into carbon atoms, and diffuse through the catalyst particle before undergoing nucleation at the tailing face. Two competing processes may occur on the catalyst particle which are either the encapsulation of carbon atoms at the leading face or diffusion of carbon atoms through the catalyst particle followed by nucleation at tailing face. The mathematical expressions representing the carbon balance at the leading face is given by equation (3) where variables r_f, r_g, r_d, and r_e represent dehydrogenation rate, gasification rate, carbon diffusion rate through catalyst particle, and formation rate of encapsulating layer respectively.

$$(dn_c/dt)_{x=0} = (r_f - r_g) - r_d - r_e \quad (3)$$

Equation (4) shows the carbon balance at the tailing face where the variables $\mathrm{r_{dift}}$, r_{nucl}, and r_{growth} represent carbon diffusion rate at tailing face, CNT nucleation rate, and CNT growth rate respectively.

$$(dn_c/dt)_{x=(2/3)dp} = r_{dift} - r_{nucl} - r_{growth} \quad (4)$$

Another similar model was provided by Yun and Dandy [82] which was later adopted in the works of Naha and co-workers [83] to describe the catalytic synthesis of CNT. The overall process of catalytic synthesis of CNT proposed by Naha et al. [83] is illustrated in Figure 2 where carbon atoms from combustion products is initially adsorbed on the surface of the catalyst particle (I). Carbon atoms on the particle surface partially diffuse into the catalyst particle (II) while the remaining carbon atoms reside on the particle surface, forming an encapsulating layer. Then carbon atoms inside the particle diffuse out of the particle at the interface between the particle and the substrate (III). Thereon, nucleation takes place in an upward direction (IV) and carbon atoms addition (V) leads to the CNT formation.

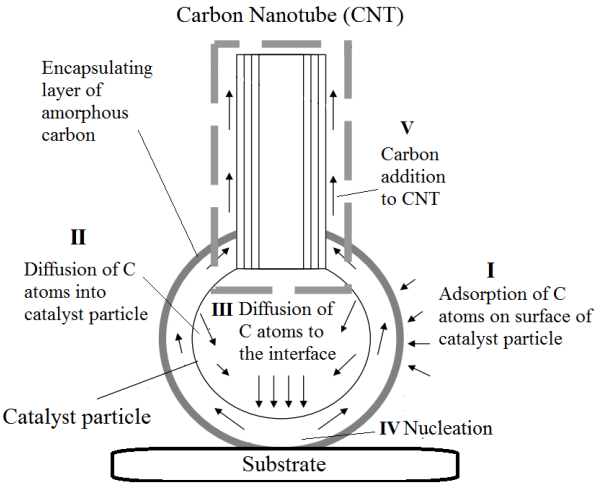

Figure 2 The overall process of catalytic formation of CNT in flames. Adapted from [83].

Equation (5) shows the rate of change of the carbon surface density on the catalyst surface where the variable $\mathrm{r_{adsorb}}$ and $\mathrm{r_{desorb}}$ denotes the rate of carbon atoms adsorption and desorption on the nanoparticle surface respectively. The rate of adsorption is a function of partial pressure and temperature while the rate of desorption is a function of temperature.

$$dn_c/dt = r_{adsorb} - r_{desorb} - r_{nucl} - r_{growth} - r_e - r_{d,out} \quad (5)$$

Both pressure and temperature are important factors in determining CNT growth. Variables r_{nucl} and $\mathrm{r_{growth}}$ represents nucleation rate and growth rate respectively, which also corresponds to the rate of critical and stable clustering of carbon atoms respectively. The clustering of carbon atoms eventually leads to CNT nucleation. The rate of formation of encapsulating layer on nanoparticle is represented by r_e to model catalyst deactivation. The diffusion rate of carbon supply out of catalyst particle for the CNT formation is represented by $\mathrm{r_{d,out}}$. The last term in equation (5) could be used to find CNT length and thus growth rate by using equation (6) where C is the carbon atom density necessary to form carbon mono layer [83].

$$L_{CNT}(t) = (1/C)\int_0^t r_{d,out}\, dt \quad (6)$$

It is worth noting that equations (5) and (6) models the growth of both SWCNT and MWCNT while

equation (2) is only applicable to the growth of SWCNT. The growth model represented by equation (5) and (6) indicates the factors resulting in increased CNT growth rate which are the increase in temperature, the increase in carbon precursor partial pressure, and the reduction in the number of CNT walls [83]. Comparing the mathematical model of Naha et al. and that of Zhang and Smith, the former is more effective in computation since it involves a single ordinary differential equation.

3.1.2 Experimental Insights for CNT Modelling in Flames

The main challenges for modelling studies are the limited experimental data for model validation and difficulties involved in the in-situ characterization of CNTs within flame environment. In flame synthesis, structural defects such as fractures, etches, and dents on CNT walls could arise due to the thermal stress [36] and electron microscopy effects [28]. Further characterization would require post-treatment process of the as-grown CNTs using strong acid solution or heat treatment to purify the CNTs [23] which may change the original form of the CNTs. The limitations mentioned above bring forth an issue of the inaccurate experimental observation during the synthesis process which will hinder the proper understanding of the physics that happen during the synthesis process. Most of the main experimental insight for the present CNT model came from a well-controlled environment in furnaces [23,25,27,84] and will be presented in this section. The main experimental data in flame synthesis which has not been incorporated in the growth rate model will be discussed for future model refinement.

The two main mechanisms of catalytic growth of CNT include the base growth which is indicated by nucleation while leaving catalyst particle attached to the substrate, and the tip growth indicated by nucleation while lifting catalyst particle away from substrate [16]. The early attempts to explain base growth and tip growth based on experiment was by Baker et al. [67] and Dai et al. [85] respectively. Figure 3 depicts both the growth mode. In the base growth mode, a graphene cap which serves as the base forms on the catalyst particle and the CNT nucleation takes place thereof as shown in Figure 3(a). Figure 3(b) shows the tip growth mode where the deposition of amorphous carbon particles on the base of catalyst particles is likely to have coerced metal particles to lift up and away from the substrate.

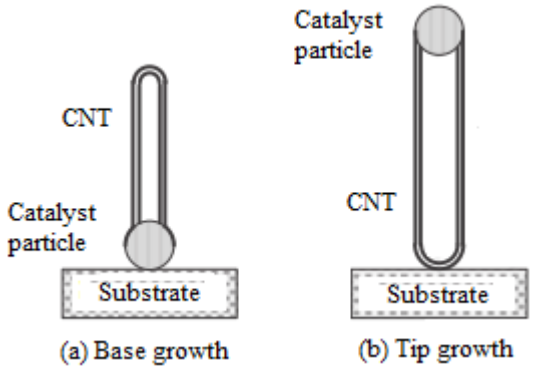

Figure 3 Illustration of CNT growth modes. Adapted from Gore and Sane [16].

In a previous study that uses molecular simulation [86], growth mechanisms are determined by the competition between the energy gained by carbon atoms in a formed nanotube and the energy that binds catalyst particles with substrate surface. If the energy gain of carbon atoms during CNT nucleation is stronger than that of the surface, the lifting of catalyst particle would take place leading to the tip growth. Alternately, insufficient energy gain will fail to detach catalyst particles from the substrate, which leads to base growth.

CNT growth rate is proportional to carbon solubility in the catalyst metal [36]. Nickel is well known to provide high carbon solubility [87] and has been deployed in numerous flame synthesis experiments. Yet, according to Xu et al. [88], bimetallic alloys provide better carbon diffusion than single metallic atom. The effects of catalyst on CNT growth is determined by the carbon diffusivity constant for a specific catalyst in the unsteady equation of carbon diffusion with a specified initial condition at the tailing face [81].

Some experiments have shown the effects of flame and catalyst parameters on CNT growth which has not been incorporated in the existing growth rate model. Previous experimental studies have shown that CNT diameter corresponds to the diameter of metal catalyst particles [89,90]. The previous growth rate model has used the CNT diameter as an input [83], but the experimental data indicates that the diameter has to be correlated with the catalyst particle diameter. This is especially true for the aerosol type catalyst which is formed from ferrocene fed [91]. CNT diameters in the range of 1-10nm for SWCNTs [21,30,39–41] and 10-100nm for MWCNT [27,29,33,43,92] in flame synthesis experiments have been reported although larger diameters of approximately 600nm has been produced in another study [93]. Nasibulin et al. [94] measured CNT diameters from electron microscopy images and statistically found that catalyst particles entrained by aerosol method is approximately 1.6 times larger than the corresponding synthesized CNTs as shown in Figure 4. On the other end, it has also been reported that

appropriately sized catalyst nanoparticles might not trigger CNT inception at all. Despite the contradiction observed, it is still a strongly held view that the catalyst and the CNT diameters are approximately the same size.

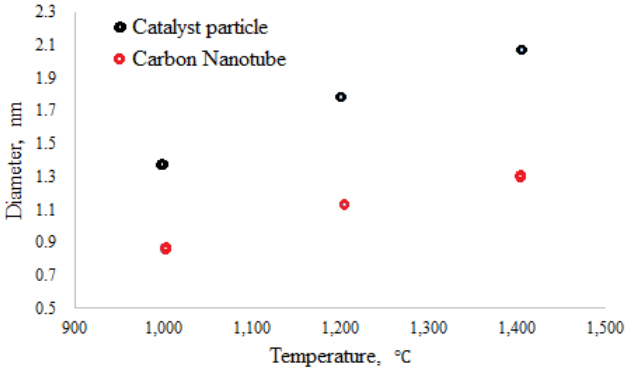

Figure 4 Comparison between the diameter of catalyst particle and that of CNT. Adapted from Nasibulin et al [94].

The variation in fuel composition was seen to influence CNT growth in few studies [25,84]. A study on diffusion flame synthesis showed that increasing methane composition from 15% to 25% improves the CNT yield. However, the yield drops at 35% methane composition, indicating that there exists limits on varying the fuel composition [25]. Another study showed that altering the oxygen composition in fuel affects the carbon nanomaterial morphology. At low oxygen content of 20%, CNT is produced while higher oxygen content between 30 and 40% yields carbon nano-onions [84].

In premixed flames, flame stretch rate κ and equivalence ratio φ are proven to influence the CNT growth. An experiment [23] showed that at high flame stretch rate ($\kappa > 1000s^{-1}$), CNT formation could be observed in a narrow range of φ between 1.7 and 1.8. Beyond this, soot formation takes place and only polluted CNTs will be formed. On the other hand, larger window of φ between 1.5 and 1.7 is available for low and moderate flame stretch ($\kappa < 1000s^{-1}$) where the MWCNT formation dominates [23]. At present, the growth rate model is still far from being able to predict the level of purity of the synthesized CNT though this capability will be crucial to explore different flame configurations for the synthesis process. The competition between CNT and soot is also an important phenomenon to be considered in the model especially if the variation of operating condition may lead to significant soot-producing region within the flame.

Several authors who conducted studies on premixed flame synthesis attempted to explain straight CNT growth mechanism at the nano-scale level. According to Hall et al. [27], straight CNT growth is likely to be assisted by the crowding mechanism which happens when CNTs produced at a substrate surface is dense enough to engender Van der Walls force to cause straight and perpendicular growth from the substrate surface [95]. Another study attributed aligned CNT formation to cleaner surface of catalyst particles due to carbon etching because such environment provides larger site for uniform carbon supply and thus straighter CNTs [34]. Nakazawa et al. [22] produced tidily aligned CNTs in double wall stagnation flow burner but the mechanism of alignment was unclear. In the electrically assisted alignment, the electric field interacts with charged dangling bond at nanotube ends to produce straight tubes [20]. Merchan-Merchan et al. [17] suggested that the alignment is assisted by a torsional force from the electrical field which acts on bent tubes. A prediction of the CNT alignment based on the competition between CNT growth and catalyst deactivation may be possible with a careful analysis of respective terms in equations (3) to (5).

The horizontal CNT growth has been shown possible but is rarely modelled. Growth mechanism of horizontally aligned CNTs differs from vertically aligned CNTs in the sense that the former growth mode occurs in parallel and along substrate surface [20]. In this case, friction between catalyst particle and substrate surface that may result in skewing the alignment should be taken into consideration. An attempt to explain the mechanism of horizontally aligned growth was done by Yu et al. [96] through the so-called raised-head model as depicted in Figure 5. According to the study, the substrate and the catalyst particles are both positively charged due to Al-O dipoles and contact potential between particle and growing CNT. The resulted repulsive interaction would refrain catalyst particle on CNT tips from dropping towards the substrate, and ensure continuous catalytic process for horizontal growth.

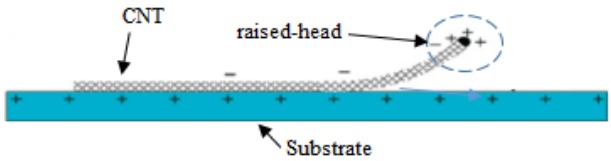

Figure 5 The horizontal growth of CNT based on the raised-head model. Adapted from Yu et al. [96].

3.1.3 Model of Catalyst Particle Formation (Aerosol Catalyst)

Early modelling of catalyst particle formation for aerosol type catalyst was done by Pope and Howard [97]. The sectional method on simultaneous particle and molecule modelling (SPAMM) based on a quasi-multi–phase model successfully computes the soot aerosol dynamics and gas-phase chemical kinetics simultaneously. In the SPAMM method, the parameters in aerosol equations and chemical kinetics coexist in one equation. This was achieved by transforming aerosol equations from the sectional approach into a form suitably appended for kinetics equation. However, the sectional method involves a

prohibitive computing cost in multi-dimensional simulation [45] and a large error due to the numerical diffusion [98,99]. These difficulties could be sidestepped using a simpler approach of moment with a presumed shape of size distribution function such as found in the work of Kuwana and co-workers [91]. The formation of aerosol catalyst particles was modelled to determine the particle size distribution throughout a CVD reactor. This approach is suitable for CFD because the presumed distribution function reduces the computational cost. However, the assumption of negligible thermophoretic effect has to be relaxed for the application of the same method in flame environment where large temperature gradient exists.

3.2 Flame-Scale Modelling

The physical phenomena at the flame are captured by using CFD that includes a detailed chemistry. A two-step computational method is mostly employed to enable the prediction of CNT growth rate where the CFD simulation is done to produce a reacting flow solution which is then used as an input to the particle scale model in a post-processing stage. This approach usually involves the assumption that changes in the flame structure such as local temperature and species concentration due to the CNT growth are negligible.

In a study by Endo and co-workers, a CFD simulation is done to determine essential parameters for CNT growth rate such as temperature, velocity, and species concentration [100]. At the post-processing stage, the rate constants for hydrocarbon molecules decomposition and the deposition rate were determined and further integrated over the growth area to find the total growth rate. The study showed that CNT growth rate increases linearly with the increment in fuel concentration [100].

Unrau et al. [51] attempted to explain the short catalyst lifetime in diffusion flame synthesis by using the computational study. The CFD is used to predict the distribution of temperature and species concentration such as C_2H_2, C_2H_4, and CO. A dispersed phase model is employed within CFD to predict the trajectory of catalyst particles. Figure 6 a) and (b) show where the trajectory of catalyst particles that is superimposed on the predicted temperature and carbon precursor fields respectively.

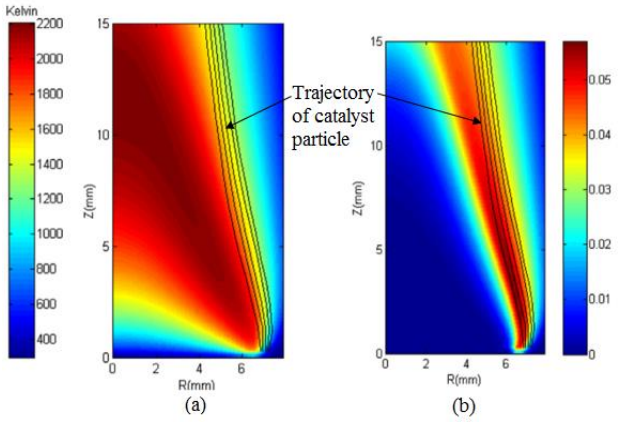

Figure 6 Particle trajectory superimposed with (a) temperature contour and (b) CO concentration contour from CFD simulation. Adapted from Unrau et al. [51].

The particle trajectories represented by the black lines were found to overlap along constant temperature and species concentration region. This suggests that the change in temperature and species concentration is not likely the factors that cause the short catalytic process. On the other hand, the change in catalyst composition is concluded to be the cause of the short catalyst lifetime through carbon encapsulation on the catalyst surface [51]. However, the conclusion has not been systematically supported due to the absence of the particle scale model to predict the change of catalyst composition in the study.

In the study of Wen et al. [45], a premixed methane-oxygen-argon flame is simulated in CHEMKIN to obtain temperature distribution, species concentration, and catalyst residence time. These simulation results were then treated as input for the particle scale model to predict the number of carbon atoms adsorbed at catalyst particle surface. Another post-processing technique was further employed using a solver based on a stochastic population balance [101] to determine CNT growth rate. Naha et al. [18] computed species concentration and temperature at different height above burner in a diffusion flame environment which are used as input in the growth rate model. In addition, the authors compared the predicted deposition rate and surface density of carbon atoms on catalyst surface with those from a CVD experimental measurement [81]. Thereon, they suggested that flame synthesis exhibits the capacity to achieve superior CNT throughput compared to CVD by comparing the duration of nucleation stage for the two synthesis methods.

Woo et al. [23] conducted a computational study of ethylene premixed flame to find temperature distribution and CO concentration in a stagnation flow burner using double wall substrate. Unlike the two-step simulation studies mentioned before, the study was not extended to the particle scale. The flame-scale simulation performed under optimal equivalence ratio and strain rate identified the region of high carbon

precursors to be up to 40 mm above the plate. The authors also reported the appropriate temperature for MWCNT formation is between 950 K and 1150 K but this conclusion has yet to be confirmed with a coupled simulation [23].

A study by Kuwana et.al [91] provided a model for iron nanoparticle formation in a CVD reactor. The temperature field in the reactor was calculated before solving the particle dynamic equation to predict the iron nanoparticle formation at the furnace entrance [100]. The nucleation and surface growth of iron nanoparticles were described by the number density and volume fraction which are implemented within a two-equation model. Ultimately, distribution of particle diameter across a CVD reactor was produced. However, it is important to note that the study assumed uniform temperature gradient [91], which needs to be refined for flame application.

Another approach to support the CNT formation modelling at flame scale is by studying the chemical kinetics side of CNT flame synthesis. Hall et al. [27] provided chemical kinetics simulation to predict the gas-phase composition for different types of fuel in premixed flames. From that, a linear relationship between carbon precursor concentration and diameter of CNTs was identified. As the hydrocarbon content in fuel source increase, so does the size of CNTs [27]. Similar relation was observed for the influence of partial pressure of CO and H_2 on the diameter of CNTs. Gopinath et al. [32] presented a 1-D chemical kinetic model for an ethylene premixed flame environment. The gas-phase species are tabulated at various heights within the post-flame region where the unburned hydrocarbon molecules is proportional to the equivalence ratio.

A similar modelling concept by Li et al. [44] provided spatial distribution of gas-phase species in a counterflow diffusion flame. The synthesis region was experimentally determined and the distribution of carbon precursors was obtained from computational works. Based on the distribution of carbon monoxide, acetylene, ethylene, ethane, and methyl radical, which fall inside the synthesis region, the carbon precursors for CNT formation are identified.

3.3 Towards a Coupled Multi-Scale Modelling of Flame Synthesis

From the review provided on the computational study of flame synthesis, it could be inferred that the coupling of particle-scale and flame scale model is majorly unidirectional. To the best of authors knowledge, two-way effect between the flame and the particle scale has never been considered before and this is mainly due to the prohibitive computational cost to resolve the two different length scales of flame and particle respectively. Particle scale and flame scale simulation are always processed independently in a one-way coupling mode. A two-way coupling method which models the two-way interaction between different scales will allow the multidimensional CFD simulation to be a helpful tool to optimize different flame configurations for CNT synthesis. This can be done with a reasonable computational cost by introducing a subgrid model which can be implemented in a surface chemistry model for a substrate based catalyst or in a dispersed phase model for an aerosol based catalyst. Then, the more advanced optimization strategies as described in section 0 can be explored computationally.

4.0 CONCLUSION

Flame synthesis is an attractive method of producing CNT due to its simple and cost effective process. Several optimization techniques from the advanced CVD research, which are possible to be adopted in flame synthesis to enhance the yield rate, the CNT quality, and the size, are presented. Among other optimization methods, the water-assisted synthesis and the catalyst-free synthesis are deemed suitable for the improvement of the purity and alignment of the synthesized CNT in flames. An accurate modelling of CNT synthesis in flames is essential to optimize growth behaviour that varies with different types of synthesis parameters such as flame temperature, carbon source, type of catalyst and substrate, and sampling region. The flame synthesis could be described in two scales which are the particle and the flame scales.

The existing particle scale models that describe the interaction between carbon precursors and catalyst particles leading to CNT growth could be coupled with the flame scale computation to allow two-way coupling between different scales. The existing mathematical model on CNT growth rate could be enhanced based on some experimental observations. Further refinement may allow the model to predict the diameter based on the size of catalyst particle. The flame scale modelling majorly involves CFD and chemical kinetics modelling to predict the flame structure such as temperature, catalyst, and species distribution. A fully coupled particle scale and reacting flow simulation will allow the optimization of the CNT synthesis in flames. However, extensive studies are required to develop such a comprehensive model.

Acknowledgement

This research was funded by the Research University Grant (RUG) with reference number PY/2014/03586 awarded by Universiti Teknologi Malaysia.

References

[1] Iijima, S. 1991. Helical microtubules of graphitic carbon. Nature. 354 (6348): 56–58.
[2] Wood, J. 2007. Putting the heat on nanotubes. Nano Today. 2 (6): 8.
[3] Zakaria, M.R., H.M. Akil, M.H.A. Kudus, and S.S.M. Saleh. 2014. Enhancement of tensile and thermal properties of

epoxy nanocomposites through chemical hybridization of carbon nanotubes and alumina. Compos. Part A Appl. Sci. Manuf. 66: 109–116.
[4] Spitalsky, Z., D. Tasis, K. Papagelis, and C. Galiotis. 2010. Carbon nanotube–polymer composites: Chemistry, processing, mechanical and electrical properties. Prog. Polym. Sci. 35 (3): 357–401.
[5] Hu, Z. and X. Lu. 2014. Carbon Nanotubes and Graphene, 2nd ed. Elsevier Ltd. 165–200.
[6] Wang, A., Y. Cheng, H. Zhang, Y. Hou, Y. Wang, and J. Liu. 2014. Effect of Multi-Walled Carbon Nanotubes and Conducting Polymer on Capacitance of Mesoporous Carbon Electrode. J. Nanosci. Nanotechnol. 14 (9): 7015–7021.
[7] Srivastava, A., A.K. Srivastava, and O.N. Srivastava. 2001. Curious aligned growth of carbon nanotubes under applied electric field. Carbon. 39 (2) 201–206.
[8] Sealy, C. 2007. Carbon nanotubes offer a crack cure. Nano Today. 2 (6): 10.
[9] Sandler, J.K., S. Pegel, M. Cadek, F. Gojny, M. van Es, J. Lohmar, W.J. Blau, K. Schulte, A.H. Windle, and M.S.P. Shaffle. 2004. A comparative study of melt spun polyamide-12 fibres reinforced with carbon nanotubes and nanofibres. Polymer. 45 (6): 2001–2015.
[10] Coleman, J.N., U. Khan, W.J. Blau, and Y.K. Gun'ko. 2006. Small but strong: A review of the mechanical properties of carbon nanotube-polymer composites. Carbon. 44 (9): 1624–1652.
[11] Sealy, C. 2013. Carbon nanotubes target tumors in two steps. Nano Today. 8 (6): 557.
[12] Liu, Z., X. Sun, N. Nakayama-Ratchford, and H. Dai. 2007. Supramolecular chemistry on water-soluble carbon nanotubes for drug loading and delivery. ACS Nano. 1 (1): 50–56.
[13] Kam, N.W.S., M. O'Connell, J.A. Wisdom, and H. Dai. 2005. Carbon nanotubes as multifunctional biological transporters and near-infrared agents for selective cancer cell destruction. Proc. Natl. Acad. Sci. U. S. A. 102 (33): 11600–11605.
[14] Han, Z.J., A.E. Rider, C. Fisher, T. van der Laan, S. Kumar, I. Levchenko, and K. Ostrikov. 2014. Carbon Nanotubes and Graphene. 2nd ed. Elsevier Ltd. 279–312.
[15] Eatemadi, A., H.D.H.K.M. Kouhi, N. Zarghami, A. Akbarzadeh, M. Abasi, Y. Hanifehpour, and S.W. Joo. 2014. Carbon nanotubes: properties, synthesis, purification, and medical applications. Nanoscale Res. Lett. 9 (393): 1–13.
[16] Gore, J.P and A. Sane. 2011. Synthesis. Characterization, Applications. InTech. 121–146.
[17] Merchan-Merchan, W., A. V. Saveliev, L. Kennedy, and W.C. Jimenez. 2010. Combustion synthesis of carbon nanotubes and related nanostructures. Prog. Energy Combust. Sci. 36 (6): 696–727.
[18] Naha, S., S. Sen, A.K. De, and I.K. Puri. 2007. A detailed model for the flame synthesis of carbon nanotubes and nanofibers. Proc. Combust. Inst. 31 (2): 1821–1829.
[19] Mittal, G., V. Dhand, K.Y. Rhee, H.J. Kim, and D.H. Jung. 2015. Carbon nanotubes synthesis using diffusion and premixed flame methods: a review. Carbon Lett. 16 (1:) 1–10.
[20] Seah, C.M., S.P. Chai, and A.R. Mohamed. 2011. Synthesis of aligned carbon nanotubes. Carbon. 49 (14): 4613–4635.
[21] Unrau, C.J., R.L. Axelbaum, P. Biswas, and P. Fraundorf. 2007. Synthesis of single-walled carbon nanotubes in oxy-fuel inverse diffusion flames with online diagnostics. Proc. Combust. Inst. 31: 1865–1872.
[22] Nakazawa, S., T. Yokomori, and M. Mizomoto. 2005. Flame synthesis of carbon nanotubes in a wall stagnation flow. Chem. Phys. Lett. 403 (1-3): 158–162.
[23] Woo, S.K., Y.T. Hong, and O.C. Kwon. 2009. Flame-synthesis limits and self-catalytic behavior of carbon nanotubes using a double-faced wall stagnation flow burner. Combust. Flame. 156 (10): 1983–1992.
[24] Vander Wal, R.L., and L.J. Hall. 2002. Ferrocene as a precursor reagent for metal-catalyzed carbon nanotubes: Competing effects. Combust. Flame. 130 (1-2): 27–36.
[25] Hou, S.S., D.H. Chung, and T.H. Lin. 2009. High-yield synthesis of carbon nano-onions in counterflow diffusion flames. Carbon. 47 (7): 938–947.
[26] Hu, W.C., S.S. Hou, and T.H. Lin. 2014. Analysis on Controlling Factors for the Synthesis of Carbon Nanotubes and Nano-Onions in Counterflow Diffusion Flames. J. Nanosci. Nanotechnol. 14 (7): 5363–5369.
[27] Hall, B., C. Zhuo, Y.A. Levendis, and H. Richter. 2011. Influence of the fuel structure on the flame synthesis of carbon nanomaterials. Carbon. 49 (11): 3412–3423.
[28] Vander Wal, R.L., T.M. Ticich, and V.E. Curtis. 2000. Diffusion flame synthesis of single-walled carbon nanotubes. Chem. Phys. Lett. 323 (3-4): 217–223.
[29] Vander Wal, R.L. and T.M. Ticich. 2001. Comparative Flame and Furnace Synthesis of Single-Walled Carbon Nanotubes. Chem. Phys. Lett. 336 (1-2): 24–32.
[30] Unrau, C.J. and R.L. Axelbaum. 2010. Gas-phase synthesis of single-walled carbon nanotubes on catalysts producing high yield. Carbon 48 (5): 1418–1424.
[31] Vander Wal, R.L. 2002. Flame synthesis of Ni-catalyzed nanofibers. Carbon. 40 (12): 2101–2107.
[32] Gopinath, P. and J. Gore. 2007. Chemical kinetic considerations for postflame synthesis of carbon nanotubes in premixed flames using a support catalyst. Combust. Flame. 151 (3): 542–550.
[33] Zhuo, C., B. Hall, H. Richter, and Y. Levendis. 2010. Synthesis of carbon nanotubes by sequential pyrolysis and combustion of polyethylene. Carbon. 48 (14): 4024–4034.
[34] Vander Wal, R.L., L.J. Hall, and G.M. Berger. 2002. The chemistry of premixed flame synthesis of carbon nanotubes using supported catalysts. Proc. Combust. Inst. 29 (1): 1079–1085.
[35] Xu, F., X. Liu, and S.D. Tse. 2006. Synthesis of carbon nanotubes on metal alloy substrates with voltage bias in methane inverse diffusion flames. Carbon. 44 (3): 570–577.
[36] Arana, C.P., I.K. Puri, and S. Sen. 2005. Catalyst influence on the flame synthesis of aligned carbon nanotubes and nanofibers. Proc. Combust. Inst. 30 (2): 2553–2560.
[37] Merchan-Merchan, W., A. V. Saveliev, and L.A. Kennedy. 2004. High-rate flame synthesis of vertically aligned carbon nanotubes using electric field control. Carbon. 42 (3): 599–608.
[38] Merchan-Merchan, W., A. V. Saveliev, and L.A. Kennedy. 2006. Flame nanotube synthesis in moderate electric fields: From alignment and growth rate effects to structural variations and branching phenomena. Carbon. 44 (15): 3308–3314.
[39] Memon, N.K., F. Xu, G. Sun, S.J.B. Dunham, B.H. Kear, and S.D. Tse. 2013. Flame synthesis of carbon nanotubes and few-layer graphene on metal-oxide spinel powders. Carbon. 63: 478–486.
[40] Memon, N.K., Multiple Inverse-Diffusion Flame Synthesis of Carbon Nanomaterials, PhD Thesis, Rutgers State University of New Jersey, 2012.
[41] Unrau, C.J., R.L. Axelbaum, and P. Fraundorf. 2010. Single-walled carbon nanotube formation on iron oxide catalysts in diffusion flames. J. Nanoparticle Res. 12 (6): 2125–2133.
[42] Lee, G.W., J. Jurng, and J. Hwang. 2004. Formation of Ni-catalyzed multiwalled carbon nanotubes and nanofibers on a substrate using an ethylene inverse diffusion flame. Combust. Flame. 139 (1-2): 167–175.
[43] Lee, G.J., J. Jurng, and J. Hwang. 2004. Synthesis of carbon nanotubes on a catalytic metal substrate by using an ethylene inverse diffusion flame. Carbon. 42 (3): 682–685.
[44] Li, T.X., K. Kuwana, K. Saito, H. Zhang, and Z. Chen. 2009. Temperature and carbon source effects on methane-air flame synthesis of CNTs. Proc. Combust. Inst. 32 (2): 1855–1861.
[45] Wen, J.Z., M. Celnik, H. Richter, M. Treska, J.B. Vander Sande, and M. Kraft. 2008. Modelling study of single walled

carbon nanotube formation in a premixed flame. J. Mater. Chem. 18 (13): 1582.
[46] Moisala, A., A.G. Nasibulin, D.P. Brown, H. Jiang, L. Khriachtchev, and E.I. Kauppinen. 2006. Single-walled carbon nanotube synthesis using ferrocene and iron pentacarbonyl in a laminar flow reactor. Chem. Eng. Sci. 61 (13): 4393–4402.
[47] Singer, J.M. and J. Grumer. 1958. Carbon Formation in Very Rich Hydrocarbon-Air Flames-I. Studies of Chemical Content, Temperature, Ionization and Particulate Matter. Symp. Combust. 7 (1): 559–569.
[48] Vander Wal, R.L. 2002. Fe-catalyzed single-walled carbon nanotube synthesis within a flame environment. Combust. Flame. 130 (1-2): 37–47.
[49] Yuan, L., T. Li, and K. Saito. 2003. Growth mechanism of carbon nanotubes in methane diffusion flames. Carbon. 41 (10): 1889–1896.
[50] Zhu, L., Y. Xiu, D.W. Hess, and C.P. Wong. 2005. Aligned carbon nanotube stacks by water-assisted selective etching. Nano Lett. 5 (12): 2641–2645.
[51] Unrau, C.J., V.R. Katta, and R.L. Axelbaum. 2010. Characterization of diffusion flames for synthesis of single-walled carbon nanotubes. Combust. Flame. 157 (9): 1643–1648.
[52] Chun Zeng, H. 2007. Ostwald Ripening: A Synthetic Approach for Hollow Nanomaterials. Curr. Nanosci. 3 (2): 177–181.
[53] Amama, P.B., C.L. Pint, L. McJilton, S.M. Kim, E. A. Stach, P.T. Murray, R.H. Hauge, and B. Maruyama. 2009. Role of water in super growth of single-walled carbon nanotube carpets. Nano Lett. 9 (1): 44–49.
[54] Yamada, T., A. Maigne, M. Yudasaka, K. Mizuno, D.N. Futaba, M. Yumura, S. Iijima, and K. Hata. 2008. Revealing the secret of water-assisted carbon nanotube synthesis by microscopic observation of the interaction of water on the catalysts. Nano Lett. 8 (12): 4288–4292.
[55] Liu, H., Y. Zhang, R. Li, X. Sun, F. Wang, Z. Ding, P. Merel, and S. Desilets. 2010. Aligned synthesis of multi-walled carbon nanotubes with high purity by aerosol assisted chemical vapor deposition: Effect of water vapor. Appl. Surf. Sci. 256 (14): 4692–4696.
[56] Li, X., A. Westwood, A. Brown, R. Brydson, and B. Rand. 2008. Water assisted synthesis of clean single-walled carbon nanotubes over a Fe2O3/Al2O3 binary aerogel catalyst. New Carbon Mater. 23 (4): 351–355.
[57] Futaba, D.N., K. Hata, T. Yamada, K. Mizuno, M. Yumura, and S. Iijima. 2005. Kinetics of Water-Assisted Single-Walled Carbon Nanotube Synthesis Revealed by a Time-Evolution Analysis. Phys. Rev. Lett. 95 (5:) 056104.
[58] Hata, K., D.N. Futaba, K. Mizuno, T. Namai, M. Yumura, and S. Iijima. 2004. Water-assisted highly efficient synthesis of impurity-free single-walled carbon nanotubes. Science. 306 (5700): 1362–1364.
[59] Yoshida, A., T. Udagawa, Y. Momomoto, H. Naito, and Y. Saso. 2013. Experimental study of suppressing effect of fine water droplets on propane/air premixed flames stabilized in the stagnation flowfield. Fire Saf. J. 58: 84–91.
[60] Zhu, Z., Y. Lu, D. Qiao, S. Bai, T. Hu, L. Li, and J. Zheng. 2005. Self-catalytic behavior of carbon nanotubes. J. Am. Chem. Soc. 127 (45): 15698–156989.
[61] Romero, P., R. Oro, M. Campos, J.M. Torralba, and R. Guzman de Villoria. 2015. Simultaneous synthesis of vertically aligned carbon nanotubes and amorphous carbon thin films on stainless steel. Carbon. 82: 31–38.
[62] Merchan-Merchan, W., A. Saveliev, L. A. Kennedy, and A. Fridman. 2002. Formation of carbon nanotubes in counter-flow, oxy-methane diffusion flames without catalysts. Chem. Phys. Lett. 354 (1-2): 20–24..
[63] Martin. I, G. Rius, P. Atienzar, L. Teruel, N. Mestres, F. Perez-Murano, H. Garcia, P. Godignon, A. Corma, and E. Lora-Tamayo. 2008. CVD oriented growth of carbon nanotubes using AlPO4-5 and L type zeolites. Microelectron. Eng. 85 (5-6): 1202–1205.
[64] Yuan, D., L. Ding, H. Chu, Y. Feng, T.P. McNicholas, and J. Liu. 2008. Horizontally aligned single-walled carbon nanotube on quartz from a large variety of metal catalysts. Nano Lett. 8 (8): 2576-2579.
[65] Liu, B., W. Ren, L. Gao, S. Li, S. Pei, C. Liu, C. Jiang, and H.M. Cheng. 2009. Metal-catalyst-free growth of single-walled carbon nanotubes. J. Am. Chem. Soc. 131 (6): 2082–2083.
[66] Simon, A., M. Seyring, S. Kamnitz, H. Richter, I. Voigt, M. Rettenmayr, and U. Ritter. 2015. Carbon nanotubes and carbon nanofibers fabricated on tubular porous Al2O3 substrates. Carbon. 90: 25–33.
[67] Baker, R.T.K., M.A. Barber, P.S. Harris, F.S. Feates, and R.J. Waite. 1972. Nucleation and Growth of Carbon Deposits from the Nickel Catalyzed Decomposition of Acetylene. J. Catal. 26 (1): 51–62.
[68] Borowiak-Palen, E., A. Bachmatiuk, M.H. Rümmeli, T. Gemming, M. Kruszynska, and R.J. Kalenczuk. 2008. Modifying CVD synthesised carbon nanotubes via the carbon feed rate. Phys. E Low-Dimensional Syst. Nanostructures. 40 (7): 2227–2230.
[69] Park, S., W. Song, Y. Kim, I. Song, S.H. Kim, S. Il Lee, S.W. Jang, and C.Y. Parkl. 2014. Effect of growth pressure on the synthesis of vertically aligned carbon nanotubes and their growth termination. J. Nanosci. Nanotechnol. 14 (7): 5216–20.
[70] Maruyama, S., R. Kojima, Y. Miyauchi, S. Chiashi, and M. Kohno. 2002. Low-temperature synthesis of high-purity single-walled carbon nanotubes from alcohol. Chem. Phys. Lett. 360 (3-4): 229–234. 2.
[71] Qian, W., H. Yu, F. Wei, Q. Zhang, and Z. Wang. 2002. Synthesis of carbon nanotubes from liquefied petroleum gas containing sulfur. Carbon. 40 (15): 2968–2970.
[72] Huang, J., Q. Zhang, F. Wei, W. Qian, D. Wang, and L. Hu. 2008. Liquefied petroleum gas containing sulfur as the carbon source for carbon nanotube forests. Carbon. 46 (2): 291–296.
[73] Zhao, J., X. Guo, Q. Guo, L. Gu, Y. Guo, and F. Feng. 2011. Growth of carbon nanotubes on natural organic precursors by chemical vapor deposition. Carbon. 49 (6): 2155–2158.
[74] Deep, A. and N. Arya. 2012. Optimization of Flame Synthesis of CNT Structures using Statistical Design of Experiments (SDOE). Int. J. Sci. Eng. Res. 3 (11): 305–312.
[75] Pan, C. and X. Xu. 2002. Synthesis of carbon nanotubes from ethanol flame. J. Mater. Sci. Lett. 21 (15): 1207–1209.
[76] Bajad, G.S., S.K. Tiwari, and R.P. Vijayakumar. 2015. Synthesis and characterization of CNTs using polypropylene waste as precursor. Mater. Sci. Eng. B. 194: 68–77.
[77] Tsai, S.H., C.T. Shiu, S.H. Lai, and H.C. Shih. 2002. Tubes on tube—a novel form of aligned carbon nanotubes. Carbon. 40 (9): 1597–1600.
[78] Santini, C.A., P.M. Vereecken, and C. Van Haesendonck. 2012. Growth of carbon nanotube branches by electrochemical decoration of carbon nanotubes. Mater. Lett. 88: 33–35.
[79] Ngo, Q., A.M. Cassell, V. Radmilovic, J. Li, S. Krishnan, M. Meyyappan, andn C.Y. Yang. 2007. Palladium catalyzed formation of carbon nanofibers by plasma enhanced chemical vapor deposition. Carbon. 45 (2): 424–428.
[80] Liu, H. and D.S. Dandy. 1996. Nucleation Kinetics Of Diamond On Carbide-Forming Substrates During Cvd — I . Transient Nucleation Stage. J. Electrochem. Soc. 143 (3): 1104–1109.
[81] Zhang, Y. and K. Smith. 2005. A kinetic model of CH4 decomposition and filamentous carbon formation on supported Co catalysts. J. Catal. 231 (2): 354–364.
[82] Yun, J. and D.S. Dandy. 2005. A kinetic model of diamond nucleation and silicon carbide interlayer formation during chemical vapor deposition. Diam. Relat. Mater. 14 (8): 1377–1388.
[83] Naha, S. and I.K. Puri. 2008. A model for catalytic growth of carbon nanotubes. J. Phys. D. Appl. Phys. 41 (6): 065304.

[84] Hou, S.S., W.C. Huang, and T.H. Lin. 2012. Flame synthesis of carbon nanostructures using mixed fuel in oxygen-enriched environment. J. Nanoparticle Res. 14 (11): 1–11.
[85] Dai, H., A.G. Rinzler, P. Nikolaev, A. Thess, D.T. Colbert, and R.E. Smalley. 1996. Single-wall nanotubes produced by metal-catalyzed disproportionation of carbon monoxide. Chem. Phys. Lett. 260 (3-4): 471–475.
[86] Banerjee, S., S. Naha, and I.K. Puri. 2008. Molecular simulation of the carbon nanotube growth mode during catalytic synthesis. Appl. Phys. Lett. 92 (23): 2006–2009.
[87] Lander, J.J., H.E. Kern, and A.L. Beach. 1952. Solubility and Diffusion Coefficient of Carbon in Nickel: Reaction Rates of Nickel-Carbon Alloys with Barium Oxide. J. Appl. Phys. 23 (12): 1305.
[88] Xu, F., H. Zhao, and S.D. Tse. 2007. Carbon nanotube synthesis on catalytic metal alloys in methane/air counterflow diffusion flames. Proc. Combust. Inst. 31 (2): 1839–1847.
[89] Cheung, C.L., A. Kurtz, H. Park, and C.M. Lieber. 2002. Diameter-controlled synthesis of carbon nanotubes. J. Phys. Chem. B. 106 (10): 2429–2433.
[90] Michalkiewicz, B. and J. Majewska. 2014. Diameter-controlled carbon nanotubes and hydrogen production. Int. J. Hydrogen Energy. 39 (9): 4691–4697.
[91] Kuwana, K. and K. Saito. 2005. Modeling CVD synthesis of carbon nanotubes: Nanoparticle formation from ferrocene. Carbon. 43 (10): 2088–2095.
[92] Hou, S.S., D.H. Chung, and T.H. Lin. 2009. Flame synthesis of carbon nanotubes in a rotating counterflow. J. Nanosci. Nanotechnol. 9 (8): 4826–4833.
[93] Manciu, F.S., J. Camacho, and A.R. Choudhuri. 2008. Flame synthesis of multi-walled carbon nanotubes using CH_4-H_2 fuel blends. Fullerenes, Nanotub. Carbon Nanostructures. 16 (4): 231–246.
[94] Nasibulin, A.G., P. V. Pikhitsa, H. Jiang, and E.I. Kauppinen. 2005. Correlation between catalyst particle and single-walled carbon nanotube diameters. Carbon. 43 (11): 2251–2257.
[95] Chen, L.C., C.Y. Wen, C.H. Liang, W.K. Hong, K.J. Chen, H.C. Cheng, C.S. Shen, C.T. Wu, and K.H. Chen. 2002. Controlling Steps During Early Stages of the Aligned Growth of Carbon Nanotubes Using Microwave Plasma Enhanced Chemical Vapor Deposition. Adv. Funct. Mater. 12 (10): 687–692.
[96] Yu, Q., G. Qin, H. Li, Z. Xia, Y. Nian, and S.S. Pei. 2006. Mechanism of horizontally aligned growth of single-wall carbon nanotubes on R-plane sapphire. J. Phys. Chem. B. 110 (45): 22676–22680.
[97] Pope, C.J. and J.B. Howard. 1997. Simultaneous Particle and Molecule Modeling (SPAMM): An Approach for Combining Sectional Aerosol Equations and Elementary Gas-Phase Reactions. Aerosol Sci. Technol. 27 (1): 73–94.
[98] Ramponi, R. and B. Blocken. 2012. CFD simulation of cross-ventilation flow for different isolated building configurations: Validation with wind tunnel measurements and analysis of physical and numerical diffusion effects. J. Wind Eng. Ind. Aerodyn. 104-106: 408–418.
[99] Mitrakos, D., E. Hinis, and C. Housiadas. 2007. Sectional Modeling of Aerosol Dynamics in Multi-Dimensional Flows. Aerosol Sci. Technol. 41 (12): 1076–1088.
[100] Endo, H., K. Kuwana, K. Saito, D. Qian, R. Andrews, and E.A. Grulke. 2004. CFD prediction of carbon nanotube production rate in a CVD reactor. Chem. Phys. Lett. 387 (4-6): 307–311.
[101] Celnik, M., R. West, N. Morgan, M. Kraft, A. Moisala, J. Wen, W. Green, and H. Richter. 2008. Modelling gas-phase synthesis of single-walled carbon nanotubes on iron catalyst particles. Carbon. 46 (3): 422–433.